

## Exotic Multigap Structure in $\text{UPt}_3$ Unveiled by a First-Principles Analysis

Takuya Nomoto<sup>1,\*</sup> and Hiroaki Ikeda<sup>2</sup>

<sup>1</sup>*Department of Physics, Kyoto University, Kyoto 606-8502, Japan*

<sup>2</sup>*Department of Physics, Ritsumeikan University, Kusatsu 525-8577, Japan*

(Received 13 March 2016; published 17 November 2016)

A heavy-fermion superconductor  $\text{UPt}_3$  is a unique spin-triplet superconductor with multiple superconducting phases. Here, we provide the first report on a first-principles analysis of the microscopic superconducting gap structure. We find that the promising gap structure is an unprecedented  $E_{2u}$  state, which is completely different from the previous phenomenological  $E_{2u}$  models. Our obtained  $E_{2u}$  state has in-plane twofold vertical line nodes on small Fermi surfaces and point nodes with linear dispersion on a large Fermi surface. These peculiar features cannot be explained in the conventional spin 1/2 representation, but is described by the group-theoretical representation of the Cooper pairs in the total angular momentum  $j = 5/2$  space. Our findings shed new light on the long-standing problems in the superconductivity of  $\text{UPt}_3$ .

DOI: 10.1103/PhysRevLett.117.217002

Identifying the pairing state and the pairing mechanism is one of the most interesting and important issues in the field of unconventional superconductivity. In particular, spin-triplet pairing states attract much attention, since there are few examples except for the superfluid  $^3\text{He}$ . In the strongly correlated electron systems, the heavy-fermion superconductor  $\text{UPt}_3$  is one of the rare candidates for spin-triplet superconductors [1,2]. The most impressive feature of this material is the multiple superconducting phase diagram. At zero magnetic field, there appears the superconducting double transition into the *A* phase at the upper critical temperature  $T_c^+ \sim 540$  mK, and then into the *B* phase at the lower  $T_c^- \sim 490$  mK [3]. Moreover, the *C* phase appears at high field and low temperature in the  $H - T$  phase diagram [4,5]. In each phase, nodal quasi-particle excitations have been observed [6–9], and also the time-reversal symmetry breaking has been reported in the *B* phase [10–12]. In spite of these prominent features, the superconducting gap structure still remains to be solved. Many scenarios have been proposed based on the phenomenological approach so far [13–16]. Among them, the most promising gap symmetry has been widely believed to be  $E_{2u}$  models [1,17–19]. However, recent measurement of the field-angle resolved thermal transport has detected in-plane twofold oscillations in the *C* phase [20]. This result is inconsistent with the proposed  $E_{2u}$  models, because in the group-theoretical argument, it is believed that the  $E_{2u}$  models do not have such in-plane twofold symmetry. Such twofold symmetry seems to be rather compatible with the  $E_{1u}$  models proposed in Refs. [21–23]. This is also supported by the following observations. A small residual thermal conductivity [24] suggests the presence of point nodes with linear dispersion in the  $E_{1u}$  models. The Josephson effect [25] with an *s*-wave superconductor is compatible with  $E_{1u}$  planar states. Thus, recently, the  $E_{1u}$

models [21–23] have been revisited. This strongly promoted the field-angle resolved specific heat measurement. However, the complimentary measurements have not detected any signature of in-plane symmetry breaking in any phases [26]. Although this seems to contradict the result in the thermal conductivity, it is expected to be explained by considering the multiband nature of  $\text{UPt}_3$ . If the twofold vertical line nodes are located on the Fermi surface (FS) with a light band mass, then the twofold oscillations will be more remarkable in the thermal conductivity than the specific heat measurement. In order to clarify how reasonable such a plausible story is, the microscopic analysis of superconductivity including the electronic structure in  $\text{UPt}_3$  is worth consideration [27–29]. In this regard, recent progress on the first-principles theoretical approach allows us to investigate the gap structure microscopically even in the complicated band structure like the heavy-fermion compounds [30–32].

In this Letter, we provide the first report on a microscopic theory of superconductivity in  $\text{UPt}_3$  based on the first-principles approach. Generally, it is difficult to exactly evaluate the effect of strong electron correlation in *f*-electron materials. Instead, we study probable candidates of gap functions based on the Fermi-liquid picture as a first step to understanding unconventional superconductivity in  $\text{UPt}_3$  [33]. We find that the promising gap structure is an unprecedented  $E_{2u}$  pairing state, which is supported by the  $j = 5/2$  representation of Cooper pairs, instead of conventional pseudospin representations. Its nodal structure is completely different on each FS: the point nodes with linear dispersion in the large hole FS, and the twofold vertical line nodes in small electron FSs. These features are not expected in the well-known phenomenological  $E_{2u}$  model. The low-energy nodal excitations are similar to those in the  $E_{1u}$  model rather than the previous  $E_{2u}$  model. The peculiar

properties can give a comprehensive explanation for the above-mentioned experimental observations, including the seemingly inconsistent result between the thermal conductivity and specific-heat measurement. Thus, the exotic  $E_{2u}$  gap structure is the most promising pairing state in the superconductivity of  $\text{UPt}_3$ .

*Fermi surface and model Hamiltonian.*—In studying the superconductivity of  $\text{UPt}_3$ , the itinerant  $5f$  model is considered to be a good starting point, since the Fermi surface in the first-principles calculations has been partially supported by the de Haas–van Alphen measurements [35,36]. Following the previous studies [30,31], we here figure out the magnetic fluctuations in  $\text{UPt}_3$ , based on the first-principles theoretical approach.

First of all, using the WIEN2k package [37], we calculate the electronic structure of  $\text{UPt}_3$ , and then construct an effective tight-binding model [38] in the Wannier bases using the WIEN2WANNIER interface [40] and the WANNIER90 code [41]. Here, we employ the space group  $P6_3/mmc$ , which holds the in-plane sixfold rotational symmetry. Note that the so-called symmetry-breaking term is not included [42,43]. Our model Hamiltonian is composed of 120 Wannier bases, containing  $U(5f)$ ,  $U(6d)$ ,  $\text{Pt}(5d)$ ,  $\text{Pt}(6s)$  orbitals and spin degrees of freedom. These bases are transformed into the bases of the total angular momentum  $j$ . In this case, due to the moderate spin-orbit coupling, the orbital components of the bands crossing the Fermi level are dominated by the  $j = 5/2$  multiplet of  $U(5f)$  orbitals, and the  $j = 7/2$  multiplet is located at much higher position.

The obtained FS is illustrated in Fig. 1. Colors on the FS, red, green, and blue, correspond to each weight of

$j_z = \pm 5/2$ ,  $\pm 3/2$ , and  $\pm 1/2$  components, respectively. The FS topology is well consistent with the previous studies [2,44,45]. The FSs of Figs. 1(b) and 1(c) have a large contribution to the density of states (DOS) at the Fermi level. Here, we realize that each FS possesses relatively separated orbital components, especially, the small FSs in Figs. 1(d) and 1(e) roughly involve only the  $j_z = \pm 3/2$  component. This characteristic feature is the key to the emergence of the unprecedented  $E_{2u}$  gap structure as discuss below.

*Magnetic fluctuations.*—Next, we study the magnetic fluctuations in the model Hamiltonian, including the on-site Hubbard-type repulsions,  $U$ ,  $U'$ ,  $J$ ,  $J'$  between  $5f$  electrons, where  $U$  is the intraorbital Coulomb repulsion,  $U'$  the interorbital one,  $J$  the Hund's coupling, and  $J'$  the pair hopping interaction. Figure 2 depicts the wave-vector dependence of the magnetic fluctuations [38]. We find that the most dominant fluctuations are located at  $\mathbf{Q} = (0, 0, 1)$  and  $(1, 0, 0)$ . The  $\mathbf{Q}$  vector corresponds to the antiparallel alignment of the magnetic moment of two  $U$  atoms in the unit cell. This is well consistent with the observed dispersive magnetic excitations by inelastic neutron scattering measurements [46,47]. On the other hand, the presence of the subdominant peaks at  $\mathbf{Q} = (0, 0, 1/2)$  and  $(1, 0, 1/2)$  may correspond to the fragile magnetic phase transition at  $T_N \approx 5$  K [48–50]. Indeed, this subdominant fluctuation is much enhanced within random phase approximation. However, it needs further investigations along with a problem of magnetic anisotropy. The magnetic anisotropy of the uniform susceptibility is slightly Ising type,  $\chi_{\parallel}(0) \gtrsim \chi_{\perp}(0)$ . Although this is the opposite to the experimental observation, we need to consider the large contribution from the localized  $f$ -electron part due to the strong electron correlations in the heavy fermion systems. This is a challenging issue in the future, and beyond the scope of this Letter.

*Superconductivity.*—Now, let us proceed to a study of the superconducting gap structure. Possible candidates can

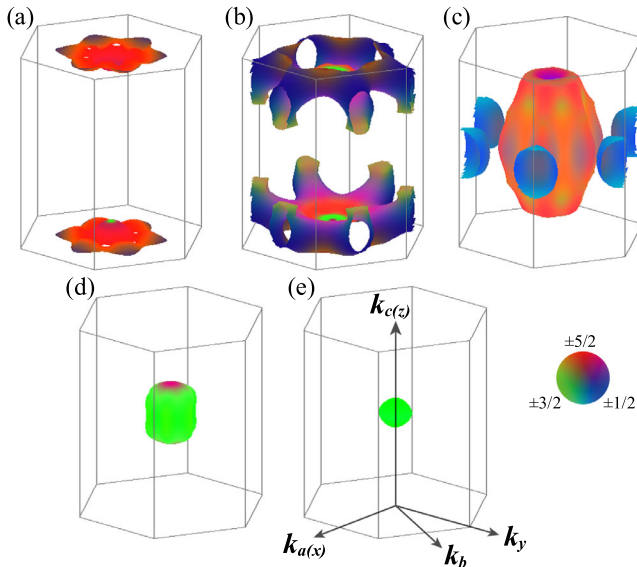


FIG. 1. Orbital-resolved Fermi surfaces in our tight-binding model  $H_0$ , obtained by the first-principles calculations. The colors correspond to the weight of the  $j_z$  component in the total angular momentum  $j = 5/2$  space. In the text, (a)–(e) are referred to as bands 1–5, respectively.

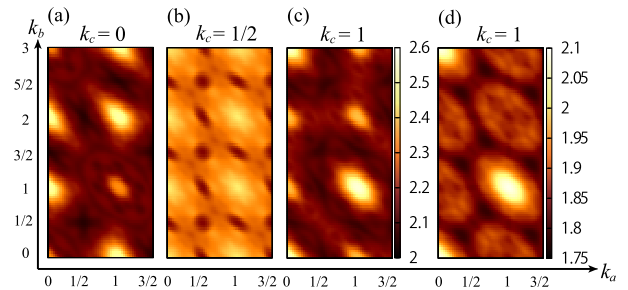


FIG. 2. Magnetic structure of the bare susceptibilities. (a)–(c) show the magnetic susceptibilities parallel to the  $c$  axis,  $\chi_{\parallel}(k_a, k_b, k_c)$ , in  $k_c = 0, 1/2$ , and  $1$  plane. Here,  $k_a$ ,  $k_b$ , and  $k_c$  are measured in units of the reciprocal lattice vectors. (d) shows the magnetic susceptibility perpendicular to the  $c$  axis,  $\chi_{\perp}(k_a, k_b, k_c)$ , in the  $k_c = 1$  plane. The difference between (c) and (d) corresponds to the magnetic anisotropy.

be obtained by calculating the linearized gap equation at around  $T_c$ .

$$\lambda \Delta_{\ell m}(k) = \sum_{k'} \sum_{\ell' \ell'' m' m''} V_{\ell \ell', m' m''}(k - k') \times \mathcal{G}_{\ell' \ell''}(k') \mathcal{G}_{m' m''}(-k') \Delta_{\ell'' m''}(k'), \quad (1)$$

where  $\Delta_{\ell m}(k)$  and  $\mathcal{G}_{\ell m}(k)$  are the  $j$ -based gap functions and one-particle Green's functions, and also  $\ell$  and  $m$  denote  $j_z$  components of each U atom [38]. The maximum eigenvalue  $\lambda$  equals to 1 at  $T_c$ . Here, the pairing interaction  $V_{\ell \ell', m' m''}(k - k')$  is estimated within the second-order perturbation theory [51]. It leads to an asymptotically exact weak-coupling solution. In this case, as shown in Fig. 3, we obtain two types of predominant spin-triplet pairing states with two dimensional representation  $E_{1u}$  and  $E_{2u}$ . This means that the present microscopic theory supports the phenomenological candidates. In our calculations, the  $E_{2u}$  state is more dominant than the  $E_{1u}$  state over a wide parameter range. From these results, we conclude that the most promising candidate for the pairing state of UPT<sub>3</sub> is the  $E_{2u}$  odd-parity state.

Next, let us elucidate the detailed microscopic structure of these pairing states. In Fig. 4, we show the superconducting gap amplitude [38] on each FS of bands 1, 3, and 4. Deep blue corresponds to the gap nodes and/or minima. Slight fluctuation of colors is attributed to the exemplification of the Blount's theorem [52] and some numerical errors. Strictly speaking, the Blount's theorem says that the symmetry-protected line nodes cannot exist in odd-parity representation except for a rare case as discussed later. Therefore, when we do not single out a specific basis function as in the present calculations, the line nodes appear just as "pseudo" line nodes, where the gap amplitude is not exact zero. Hereafter, we call the "pseudo" line nodes by the line nodes.

It is instructive to start with the  $E_{1u}$  state. In such a two-dimensional representation, there are two kinds of basis functions. Illustrated in Figs. 4(a)–4(c) is one possible gap

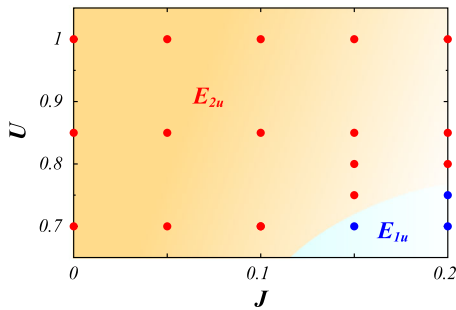


FIG. 3. Superconducting phase diagram for the intraorbital on-site repulsion  $U$  and Hund's coupling  $J$ . The unit of energy is eV [51]. Here, we set the interorbital interaction  $U' = U$  and the pair hopping  $J' = J$ .  $E_{2u}$  state is predominant over the wide range. Even if assuming SU(2) condition,  $U = U' + 2J$ , the tendency is almost unchanged.

structure in the  $E_{1u}$  state. Another one is not shown here. Roughly speaking, the nodal structure on the FS at around the  $\Gamma$  point in Fig. 4(b) is the  $f$ -wave pairing state having one vertical line node and two horizontal line nodes at  $k_z \neq 0$  plane. This nodal structure is identical to the  $E_{1u}$  model, which has been proposed based on the observations in the field-angle resolved thermal conductivity. Since the relevant FS has a large DOS, the in-plane twofold oscillation should be detected also in any experimental observations. However, this is incompatible with the observation in the field-angle resolved specific heat measurement [26].

Furthermore, let us consider the gap structure in the  $E_{2u}$  state in Figs. 4(d)–4(f). Surprisingly, we find that the nodal feature is completely different on each FS: horizontal nodes in Fig. 4(d), point nodes at the top of FS in Fig. 4(e), and in-plane twofold vertical line nodes in Fig. 4(f). These nodal structures are completely different from those of the previous phenomenological  $E_{2u}$  models despite the same irreducible representation.

Generally, the superconducting order parameter is classified by irreducible representations of the point group symmetry, since the linearized gap equation is separable for each representation. For strong SOC, symmetry operations act on all the spin, orbital, and wave-vector degrees of freedom. If we as usual consider a spin one-half Fermion system without any other internal degrees of freedom, then following Refs. [2] and [53], we can see that the only possible type of  $p$ -wave gap function in  $E_{2u}$  representation is  $(\hat{d}_x k_x - \hat{d}_y k_y, -\hat{d}_x k_y - \hat{d}_y k_x)$  in the  $\mathbf{d}$ -vector notation. This minimal gap function has only a point node at the top of FS. Even if considering its higher harmonics, there does

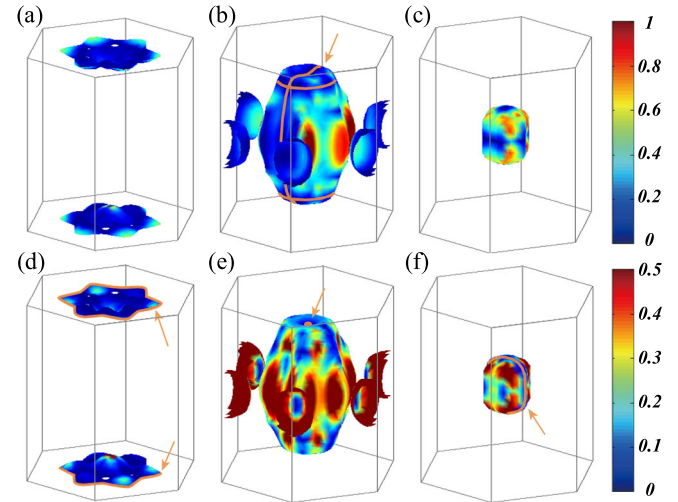


FIG. 4. Superconducting gap amplitude,  $\sum_{n'=\pm n} |\bar{\Delta}_{nn'}(\mathbf{k})|^2$ , on the FSs of band 1, band 3, and band 4 [38], where  $\bar{\Delta}_{nn'}(\mathbf{k}) = \sum_{\ell m} u_{\ell n}(\mathbf{k}) \Delta_{\ell m} u_{m n'}^*(-\mathbf{k})$  with the unitary matrix  $u_{\ell n}(\mathbf{k})$  diagonalizing  $H_0$ .  $n' = \pm n$  means a sum of the Kramers degeneracy for band  $n$ . (a)–(c) correspond to the  $E_{1u}$  state, and (d)–(f) the  $E_{2u}$  state. Line and point nodes colored by orange are pointed by arrows.

not appear any twofold vertical line nodes. Therefore, it has been widely believed that in the  $D_{6h}$  point group, twofold vertical line nodes are allowed only in  $E_{1u}$  representation, and generally forbidden in  $E_{2u}$  representation [53]. In this regard, our  $E_{2u}$  gap structure seems to be very curious. However, in our case, we need to consider the Cooper pairs

in the effective  $j = 5/2$  space [54–56], instead of conventional pseudospin  $1/2$ . Such an extension can be performed with the help of the projection operator method as in the case of spin  $1/2$ . Thereby, we find that for the minimal  $p$ -wave pairing, one of two bases in the  $E_{2u}$  representation can be described as follows,

$$\Delta_1(\mathbf{k}) = \begin{pmatrix} j_z = 5/2 & 3/2 & 1/2 & -1/2 & -3/2 & -5/2 \\ c_1(k_x - ik_y) & c_2k_z & c_3k_x + c_4ik_y & c_5k_z & c_6(k_x + ik_y) & 0 \\ c_2k_z & c_7k_x + c_8ik_y & c_9k_z & c_{10}(k_x + ik_y) & 0 & c_6(-k_x + ik_y) \\ c_3k_x + c_4ik_y & c_9k_z & c_{11}(k_x + ik_y) & 0 & c_{10}(-k_x + ik_y) & c_5k_z \\ c_5k_z & c_{10}(k_x + ik_y) & 0 & c_{11}(-k_x + ik_y) & c_9k_z & -c_3k_x + c_4ik_y \\ c_6(k_x + ik_y) & 0 & c_{10}(-k_x + ik_y) & c_9k_z & -c_7k_x + c_8ik_y & c_2k_z \\ 0 & c_6(-k_x + ik_y) & c_5k_z & -c_3k_x + c_4ik_y & c_2k_z & c_1(-k_x - ik_y) \end{pmatrix},$$

where  $c_i (i = 1-11)$  are material-dependent parameters. From the expressions of the second and fifth diagonal elements, we can verify that twofold vertical line nodes appear in the  $j_z = \pm 3/2$  subspace. Similarly, we find that the gap functions in the  $j_z = \pm 5/2$  or  $\pm 1/2$  subspace yield only point nodes with the linear dispersion along the  $c$  axis, and the twofold vertical line nodes are forbidden. Anomalous twofold vertical line nodes in the  $E_{2u}$  representation emerge only in the  $j_z = \pm 3/2$  space. In  $U\text{Pt}_3$ , the FSs in Figs. 1(d) and 1(f) involve plenty of the  $j_z = \pm 3/2$  component. Thus, it is natural that twofold vertical line nodes emerge in these FSs even in  $E_{2u}$  gap symmetry. Moreover, it should be noted that these FSs have a light band mass. In this case, it can be expected that the in-plane twofold oscillation in the field-angle resolved measurements is more prominent in the thermal conductivity than in the specific heat measurements. This can provide an explanation for the seemingly inconsistent observations between these measurements. In addition, since the FS around  $\Gamma$  in Fig. 1(c) is almost composed of  $j_z = \pm 5/2$ , we recognize that the point nodes observed in Fig. 4(e) have linear dispersion, which can be consistent with the small residual thermal conductivity [24].

In order to understand more about this unprecedented  $E_{2u}$  gap structure, let us dissect the superconducting gap structure in Fig. 4(f). Although the  $p$ -wave line nodes on the  $k_x = 0$  plane are remarkable as mentioned above, we can realize additional gap minima on the  $k_y = 0$  and  $k_z = 0$  planes. This implies a mixing of the  $f$ -wave component with the form of  $k_x k_y k_z \hat{d}_z$ , which is indeed allowed in the group-theoretical arguments. Therefore, roughly speaking, the gap structure in Fig. 4(f) can be described as a linear combination between the  $p$ -wave  $k_x \hat{d}_x$  and  $f$ -wave  $k_x k_y k_z \hat{d}_z$  in the  $\mathbf{d}$ -vector representation in the  $j_z = \pm 3/2$

space. Following Ref. [1], it will be natural that this  $p + f$ -wave gap function shows vertical line nodes in the  $A$  and  $C$  phase, and breaks the time-reversal symmetry in the  $B$  phase. Furthermore, under the applied field parallel to the  $c$  axis, the Pauli-limiting behavior will be expected in the upper critical field. Although such suppression has been observed experimentally, we need further investigations, considering the magnetic anisotropy.

Finally, let us comment on the horizontal line nodes at  $k_z = \pm 1$  in Fig. 4(d). As mentioned above, in an ordinary case, there are only point nodes in the  $E_{2u}$  representation. However, in the nonsymmorphic system like  $U\text{Pt}_3$ , there exists additional  $C_2$  screw symmetry, which protects the horizontal line nodes. The symmetry-protected line nodes are known as one of the exceptions to the Blount's theorem [57]. In the actual situation, however, the interesting line nodes are simply lifted, or slightly shifted from the  $k_z = \pm 1$  plane, due to the presence of a weak symmetry-breaking term [43,50]. This is a challenge for the future.

*Conclusion.*—Based on the advanced first-principles theoretical approach, we clarify the microscopic gap structure in the heavy-fermion superconductor  $U\text{Pt}_3$ . We find that the obtained antiferromagnetic fluctuations with  $\mathbf{Q} = (0, 0, 1)$  and  $(1, 0, 0)$ , which are consistent with the neutron scattering measurements, lead to the spin-triplet pairing states with  $E_{1u}$  and  $E_{2u}$  representations in the  $D_{6h}$  space group. The obtained  $E_{1u}$  gap structure is consistent with the phenomenological  $f$ -wave pairing state. On the other hand, the latter  $E_{2u}$  state, having nodal structure different for each band, is distinct from the well-known  $E_{2u}$  models. In particular, the in-plane twofold vertical line nodes emerge on the small FS, which can consistently explain the field-angle resolved measurements in both the thermal conductivity and the specific heat. Such a peculiar

feature cannot be explained in the conventional pseudospin representation, but is described by the group-theoretical representation of the Cooper pairs in the  $j = 5/2$  space. Furthermore, the study of magnetic anisotropy and the mixture of  $p$  wave and  $f$  wave with different  $\mathbf{d}$  vectors [58] can provide a clue to understanding the remaining problems of the Pauli limiting of the upper critical field [17,26,59] and the anomalous behavior of the Knight shift [60], and so on. These will be interesting issues in the future, together with the understanding of the multiple superconducting phases. Thus, our findings shed new light on the long-standing problems in the superconductivity of  $\text{UPt}_3$ .

We acknowledge Y. Yanase, K. Machida, and K. Hattori for valuable discussions, and K. Izawa and Y. Machida for their recent data and helpful discussions. This work was partially supported by JSPS KAKENHI Grants No. 15H05745, No. 15H02014, No. 15J01476, No. 16H01081, and No. 16H04021.

\*nomoto.takuya@sphys.kyoto-u.ac.jp

- [1] J. A. Sauls, *Adv. Phys.* **43**, 113 (1994).
- [2] R. Joynt and L. Taillefer, *Rev. Mod. Phys.* **74**, 235 (2002).
- [3] R. A. Fisher, S. Kim, B. F. Woodfield, N. E. Phillips, L. Taillefer, K. Hasselbach, J. Flouquet, A. L. Giorgi, and J. L. Smith, *Phys. Rev. Lett.* **62**, 1411 (1989).
- [4] G. Bruls, D. Weber, B. Wolf, P. Thalmeier, B. Lüthi, A. de Visser, and A. Menovsky, *Phys. Rev. Lett.* **65**, 2294 (1990).
- [5] S. Adenwalla, S. W. Lin, Q. Z. Ran, Z. Zhao, J. B. Ketterson, J. A. Sauls, L. Taillefer, D. G. Hinks, M. Levy, and B. K. Sarma, *Phys. Rev. Lett.* **65**, 2298 (1990).
- [6] B. S. Shivaram, Y. H. Jeong, T. F. Rosenbaum, and D. G. Hinks, *Phys. Rev. Lett.* **56**, 1078 (1986).
- [7] J. P. Brison, N. Keller, P. Lejay, J. L. Tholence, A. Huxley, N. Bernhoeft, A. I. Buzdin, B. Fåk, J. Flouquet, L. Schmidt *et al.*, *J. Low Temp. Phys.* **95**, 145 (1994).
- [8] B. Lussier, B. Ellman, and L. Taillefer, *Phys. Rev. B* **53**, 5145 (1996).
- [9] H. Suderow, J. P. Brison, A. Huxley, and J. Flouquet, *Phys. Rev. Lett.* **80**, 165 (1998).
- [10] G. M. Luke, A. Keren, L. P. Le, W. D. Wu, Y. J. Uemura, D. A. Bonn, L. Taillefer, and J. D. Garrett, *Phys. Rev. Lett.* **71**, 1466 (1993).
- [11] J. D. Strand, D. J. Bahr, D. J. Van Harlingen, J. P. Davis, W. J. Gannon, and W. P. Halperin, *Science* **328**, 1368 (2010).
- [12] E. R. Schemm, W. J. Gannon, C. M. Wishne, W. P. Halperin, and A. Kapitulnik, *Science* **345**, 190 (2014).
- [13] E. I. Blount, C. M. Varma, and G. Aeppli, *Phys. Rev. Lett.* **64**, 3074 (1990).
- [14] D. F. Agterberg and M. B. Walker, *Phys. Rev. B* **51**, 8481 (1995).
- [15] M. E. Zhitomirsky and K. Ueda, *Phys. Rev. B* **53**, 6591 (1996).
- [16] P. L. Krotkov and V. P. Mineev, *Phys. Rev. B* **65**, 224506 (2002).
- [17] C. H. Choi and J. A. Sauls, *Phys. Rev. B* **48**, 13684 (1993).
- [18] J. A. Sauls, *J. Low Temp. Phys.* **95**, 153 (1994).
- [19] M. J. Graf, S.-K. Yip, and J. A. Sauls, *Phys. Rev. B* **62**, 14393 (2000).
- [20] Y. Machida, A. Itoh, Y. So, K. Izawa, Y. Haga, E. Yamamoto, N. Kimura, Y. Onuki, Y. Tsutsumi, and K. Machida, *Phys. Rev. Lett.* **108**, 157002 (2012).
- [21] K. Machida and M. A. Ozaki, *Phys. Rev. Lett.* **66**, 3293 (1991).
- [22] K. Machida, T. Ohmi, and M. A. Ozaki, *J. Phys. Soc. Jpn.* **62**, 3216 (1993).
- [23] Y. Tsutsumi, K. Machida, T. Ohmi, and M. A. Ozaki, *J. Phys. Soc. Jpn.* **81**, 074717 (2012).
- [24] K. Izawa, Y. Machida, A. Itoh, Y. So, K. Ota, Y. Haga, E. Yamamoto, N. Kimura, Y. Onuki, Y. Tsutsumi, and K. Machida, *J. Phys. Soc. Jpn.* **83**, 061013 (2014).
- [25] J. Gouchi, A. Sumiyama, G. Motoyama, A. Yamaguchi, N. Kimura, E. Yamamoto, Y. Haga, and Y. Onuki, *J. Phys. Soc. Jpn.* **81**, 113701 (2012).
- [26] S. Kittaka, K. An, T. Sakakibara, Y. Haga, E. Yamamoto, N. Kimura, Y. Onuki, and K. Machida, *J. Phys. Soc. Jpn.* **82**, 024707 (2013).
- [27] M. R. Norman, *Phys. Rev. Lett.* **59**, 232 (1987).
- [28] W. Putikka and R. Joynt, *Phys. Rev. B* **37**, 2372 (1988).
- [29] M. R. Norman, *Phys. Rev. Lett.* **72**, 2077 (1994).
- [30] H. Ikeda, M.-T. Suzuki, R. Arita, T. Takimoto, T. Shibauchi, and Y. Matsuda, *Nat. Phys.* **8**, 528 (2012).
- [31] H. Ikeda, M.-T. Suzuki, and R. Arita, *Phys. Rev. Lett.* **114**, 147003 (2015).
- [32] T. Nomoto and H. Ikeda, *Phys. Rev. B* **90**, 125147 (2014).
- [33] In  $\text{UPt}_3$ , the observed quantum oscillation can be roughly explained by the Fermi surface of the GGA band. This implies that the Fermi surface in the renormalized band is not so drastically different from that in the original GGA band. Therefore, we can expect that momentum dependence of the pairing interaction and the obtained gap structure will hardly change even considering the correlation effect [34]. Hereafter, the correlation effect is considered only through the mass renormalization factor, which is  $z \sim 1/20$  from the specific heat coefficient. The interplay between the electron correlation and superconductivity will be an interesting issue in future.
- [34] Y. Yanase, T. Jujo, T. Nomura, H. Ikeda, T. Hotta, and K. Yamada, *Phys. Rep.* **387**, 1 (2003).
- [35] L. Taillefer and G. G. Lonzarich, *Phys. Rev. Lett.* **60**, 1570 (1988).
- [36] N. Kimura, T. Komatsubara, D. Aoki, Y. Onuki, Y. Haga, E. Yamamoto, H. Aoki, and H. Harima, *J. Phys. Soc. Jpn.* **67**, 2185 (1998).
- [37] P. Blaha *et al.* WIEN2K package, <http://www.wien2k.at>.
- [38] See Supplemental Material at <http://link.aps.org/supplemental/10.1103/PhysRevLett.117.217002>, which includes Ref. [39], for details.
- [39] J. P. Perdew, K. Burke, and M. Ernzerhof, *Phys. Rev. Lett.* **77**, 3865 (1996).
- [40] J. Kuneš, R. Arita, P. Wissgott, A. Toschi, H. Ikeda, and K. Held, *Comput. Phys. Commun.* **181**, 1888 (2010).
- [41] N. Marzari and D. Vanderbilt, *Phys. Rev. B* **56**, 12847 (1997); I. Souza, N. Marzari, and D. Vanderbilt, *Phys. Rev. B* **65**, 035109 (2001); A. A. Mostofi, J. R. Yates, Y.-S. Lee, I. Souza, D. Vanderbilt, and N. Marzari, *Comput. Phys. Commun.* **178**, 685 (2008).

- [42] P. A. Midgley, S. M. Hayden, L. Taillefer, B. Bogenberger, and H. v. Löhneysen, *Phys. Rev. Lett.* **70**, 678 (1993).
- [43] D. A. Walko, J.-I. Hong, T. V. Chandrasekhar Rao, Z. Wawrzak, D. N. Seidman, W. P. Halperin, and M. J. Bedzyk, *Phys. Rev. B* **63**, 054522 (2001).
- [44] M. R. Norman, R. C. Albers, A. M. Boring, and N. E. Christensen, *Solid State Commun.* **68**, 245 (1988).
- [45] G. J. McMullan, P. M. C. Rourke, M. R. Norman, A. D. Huxley, N. Doiron-Leyraud, J. Flouquet, G. G. Lonzarich, A. McCollam, and S. R. Julian, *New J. Phys.* **10**, 053029 (2008).
- [46] G. Aeppli, A. Goldman, G. Shirane, E. Bucher, and M.-Ch. Lux-Steiner, *Phys. Rev. Lett.* **58**, 808 (1987).
- [47] A. I. Goldman, G. Shirane, G. Aeppli, E. Bucher, and J. Hufnagl, *Phys. Rev. B* **36**, 8523 (1987).
- [48] G. Aeppli, E. Bucher, C. Broholm, J. K. Kjems, J. Baumann, and J. Hufnagl, *Phys. Rev. Lett.* **60**, 615 (1988).
- [49] P. Frings, B. Renker, and C. Vettier, *Physica (Amsterdam)* **151B**, 499 (1988).
- [50] S. M. Hayden, L. Taillefer, C. Vettier, and J. Flouquet, *Phys. Rev. B* **46**, 8675(R) (1992).
- [51] Based on the Fermi-liquid picture, these interactions should be considered to be quasiparticle interactions, which are renormalized and much smaller than the bare values. The second-order perturbation for the renormalized interactions is valid as asymptotically an exact weak-coupling limit. Here, we focus on probable spin-triplet states emerging in this limit, although we have used a relatively large value of interactions to obtain moderate eigenvalues.
- [52] E. I. Blount, *Phys. Rev. B* **32**, 2935 (1985).
- [53] M. Sigrist and K. Ueda, *Rev. Mod. Phys.* **63**, 239 (1991).
- [54] H. Kim, K. Wang, Y. Nakajima, R. Hu, S. Ziemak, P. Syers, L. Wang, H. Hodovanets, J. D. Denlinger, P. M. R. Brydon, D. F. Agterberg, M. A. Tanatar, R. Prozorov, and J. Paglione, [arXiv:1603.03375](https://arxiv.org/abs/1603.03375).
- [55] P. M. R. Brydon, L. Wang, M. Weinert, and D. F. Agterberg, *Phys. Rev. Lett.* **116**, 177001 (2016).
- [56] T. Nomoto, K. Hattori, and H. Ikeda, [arXiv:1607.02716](https://arxiv.org/abs/1607.02716).
- [57] T. Micklitz and M. R. Norman, *Phys. Rev. B* **80**, 100506(R) (2009).
- [58] Y. Yanase, [arXiv:1606.08563](https://arxiv.org/abs/1606.08563).
- [59] B. S. Shivaram, T. F. Rosenbaum, and D. G. Hinks, *Phys. Rev. Lett.* **57**, 1259 (1986).
- [60] H. Tou, Y. Kitaoka, K. Ishida, K. Asayama, N. Kimura, Y. Onuki, E. Yamamoto, Y. Haga, and K. Maezawa, *Phys. Rev. Lett.* **80**, 3129 (1998).